

# Thermal Hall Conductivity as a Probe of Gap Structure in Multi-band Superconductors: The Case of $\text{Ba}_{1-x}\text{K}_x\text{Fe}_2\text{As}_2$

J. G. Checkelsky<sup>1,†</sup>, R. Thomale<sup>2</sup>, Lu Li<sup>1,‡</sup>, G. F. Chen<sup>3</sup>, J. L. Luo<sup>3</sup>, N. L. Wang<sup>3</sup> and N. P. Ong<sup>1</sup>

<sup>1</sup>*Department of Physics, Princeton University, Princeton, NJ 08544, USA*

<sup>2</sup>*Department of Physics, Stanford University, Stanford, CA 94305, USA*

<sup>3</sup>*Beijing National Laboratory, Institute of Physics, Chinese Academy of Sciences, Beijing 100080, China*

(Dated: October 27, 2018)

The sign and profile of the thermal Hall conductivity  $\kappa_{xy}$  gives important insights into the gap structure of multi-band superconductors. With this perspective, we have investigated  $\kappa_{xy}$  and the thermal conductivity  $\kappa_{xx}$  in  $\text{Ba}_{1-x}\text{K}_x\text{Fe}_2\text{As}_2$  which display large peak anomalies in the superconducting state. The anomalies imply that a large hole-like quasiparticle (qp) population exists below the critical temperature  $T_c$ . We show that the qp mean-free-path inferred from  $\kappa_{xx}$  reproduces the observed anomaly in  $\kappa_{xy}$ , providing a consistent estimate of a large qp population. Further, we demonstrate that the hole-like signal is consistent with a theoretical scenario where despite potentially large gap variations on the electron pockets, the minimal homogeneous gap of the superconducting phase resides at a hole pocket. Implications for probing the gap structure in the broader class of pnictide superconductors are discussed.

The discovery [1–5] of superconductivity in the iron pnictides has galvanized intense interest in this new class of superconductors. As in the cuprates, one of the key issues has been the determination of the gap symmetry [6]. While for a large class of pnictides theory has quickly converged on an  $s_{\pm}$  order parameter which changes sign between hole and electron pockets [7–11], many questions remain regarding the actual form of superconducting pairing, such as gap anisotropies, awaiting further experimental investigation [12]. Among the evidence from measurements on  $\text{Ba}_{1-x}\text{K}_x\text{Fe}_2\text{As}_2$ , nuclear magnetic resonance (NMR) relaxation experiments [13–16] appear to be consistent with a multi-gap scenario of singlet pairing, and penetration depth [17] as well as thermal conductivity [18] experiments suggest the presence of strong gap variations inducing close-to-nodal behavior. Alternatively, angle-resolved photoemission spectroscopy (ARPES) experiments [19–21] favor an isotropic multiple gap scenario, with higher confidence for the hole pockets located at  $\Gamma$  than for the electron pockets at  $M$ .

If the gap parameter  $\Delta(\mathbf{k})$  is isotropic on each FS sheet, the population of Bogoliubov quasiparticles decreases sharply below  $T_c$  ( $\mathbf{k}$  is a wave vector on the FS). By contrast, if nodes exist in  $\Delta(\mathbf{k})$  (or if  $|\Delta(\mathbf{k})|$  is strongly anisotropic), the quasiparticle (qp) population decreases quite gradually. In effective single band superconductors with unconventional gap symmetry, the thermal Hall conductivity  $\kappa_{xy}$  has proved to be a powerful probe for quasiparticles (qps). Unlike the diagonal thermal conductivity  $\kappa_{xx}$  which is the sum of the electronic term  $\kappa_e$  and the phonon term  $\kappa_{ph}$ , the off-diagonal term  $\kappa_{xy}$  is purely electronic. Together,  $\kappa_{xx}$  and  $\kappa_{xy}$  have been used to probe extensively the qp density and their lifetime in the cuprate  $\text{YBa}_2\text{Cu}_3\text{O}_y$  (YBCO) [22–24] and the heavy fermion superconductor  $\text{CeCoIn}_5$  [25, 26]. In contrast to effective single-band descriptions of the above compounds, the pnictides are manifestly multi-band superconductors with both electron and hole-like Fermi pockets. We report thermal Hall results which

connect to the following insight: *whether the thermal Hall signal is electron- or hole-like yields non-trivial information in the presence of potentially both hole-like and electron-like low-lying charge carriers.* In principle, this also applies to thermopower experiments [27], though such electrical probes are restricted to the non-superconducting state. For the pnictides, this provides valuable consistency checks of different theoretical gap scenarios, as we explicate in the following for the specific case of  $\text{Ba}_{1-x}\text{K}_x\text{Fe}_2\text{As}_2$ . There, we find theoretically that while the largest gap anisotropy exist along the electron pockets, the lowest gap resides at a hole pocket, which is consistent with our findings from thermal Hall conductivity.

To begin, we report detailed measurements of  $\kappa_{xx}(T, H)$  and  $\kappa_{xy}(T, H)$  on single crystals of  $\text{Ba}_{1-x}\text{K}_x\text{Fe}_2\text{As}_2$  in the geometry with the field  $\mathbf{H}||\hat{\mathbf{z}}||\hat{\mathbf{c}}$  and  $-\nabla T||\hat{\mathbf{x}}$ . The longitudinal and transverse temperature gradients  $\delta T_x$  and  $\delta T_y$  were measured using chromel-alumel thermocouples. The 2 crystals studied have dimensions  $2 \times 1 \times 0.1 \text{ mm}^3$ . At 10 K, the resolution achieved is  $\delta T_y \sim 10 \text{ mK}$ . Measurements of  $\kappa_{xy}$  were made to a field up to 14 T using thermocouples. To extend measurements of  $\kappa_{xx}$  below 6 K where the thermocouple sensitivity falls steeply, we used matched  $\text{RuO}_x$  micro-sensors which are very sensitive below 4 K (measurements were performed to  $H = 35 \text{ T}$ ). Electrical measurements are performed using standard 4-probe techniques using a lock-in amplifier. All measurements are performed in a vacuum atmosphere.

Figure 1(a) plots the  $T$  dependence of  $\kappa_{xx}(T, H)$  in Sample 1 with  $H = 0$  (circles) and with  $H = 35 \text{ T}$  (triangles), together with the in-plane resistivity  $\rho$  (solid curve). The curve for  $\kappa_{xx}(T, 0)$  is closely similar in Sample 2. As shown,  $\kappa_{xx}(T, 0)$  is nearly  $T$  independent between  $T_c (= 37 \text{ K})$  and 100 K. Below  $T_c$ , it rises to a broad maximum that peaks near  $\frac{1}{2}T_c$ . In a 35-Tesla field, the anomaly is almost completely suppressed. In the Boltzmann theory approach,  $\kappa_e$  from qp excitations is given

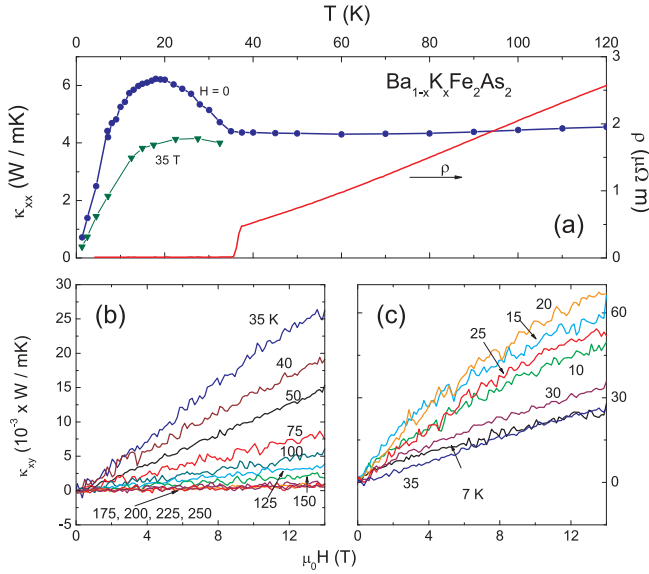


FIG. 1: (color online) (a)  $\kappa_{xx}$  of single-crystal  $\text{Ba}_{1-x}\text{K}_x\text{Fe}_2\text{As}_2$  at  $H = 0$  (circles) and at 35 T (triangles). The solid curve is the in-plane resistivity  $\rho$  in zero  $H$  ( $T_c = 37$  K).  $\kappa_{xy}$  vs.  $H$  at  $T = 250 \rightarrow 35$  K and from  $35 \rightarrow 7$  K are shown in (b) and (c), respectively. Above  $T_c$  (37 K),  $\kappa_{xy}$  is  $H$  linear up to 14 T, but as  $T$  decreases below  $T_c$ , curvature becomes increasingly apparent. At all  $T$ , the Hall signal is hole-like.

by [28, 29]

$$\kappa_e = \frac{4}{T} \sum_{\mathbf{k}} \left( -\frac{\partial f_0}{\partial E_{\mathbf{k}}} \right) E_{\mathbf{k}}^2 v_x(\mathbf{k})^2 \tau(\mathbf{k}), \quad (1)$$

where  $E_{\mathbf{k}} = \sqrt{\Delta(\mathbf{k})^2 + \epsilon_{\mathbf{k}}^2}$  is the qp energy with  $\epsilon_{\mathbf{k}}$  the normal-state energy. Here,  $\mathbf{v}(\mathbf{k})$  is the qp group velocity,  $f_0$  the Fermi-Dirac distribution and  $\tau(\mathbf{k})$  the transport relaxation time. A recent treatment of  $\kappa_{xy}$  applied to YBCO is given by Durst *et al.* [30]. Both the anomaly profile and its field suppression are similar to features seen in YBCO and CeCoIn<sub>5</sub>. In these unconventional superconductors,  $\kappa_{xx}$  also rises to a large peak near  $\frac{1}{2}T_c$ , reflecting a large qp population and a greatly enhanced (zero-field) qp mean-free-path  $\ell_0$ . By contrast,  $\kappa_{xx}$  decreases roughly linearly with  $(T_c - T)$  below  $T_c$  in the clean  $s$ -wave superconductors Pb,Hg and Sn [28, 29] (data on  $\kappa_{xy}$  are unavailable).

The curves of  $\kappa_{xy}$  vs.  $H$  at fixed  $T$  are displayed in Fig. 1(b) and 1(c). Both above and below  $T_c$ , the sign of  $\kappa_{xy}$  is positive (hole-like). Above  $T_c$ ,  $\kappa_{xy}$  is strictly linear in  $H$  (up to 14 T). As  $T$  decreases from 100 K to  $T_c$ , the slope of  $\kappa_{xy}$  vs.  $H$  increases gradually until  $T_c$ , where it undergoes a sharp increase. In the normal state,  $\kappa_{xy}$  originates from the Lorentz force acting on the charge carriers (the Hall effect is also hole-like). Below  $T_c$ , the scattering of qps from pinned vortex lines possesses a right-left asymmetry which leads to a large  $\kappa_{xy}$  [22, 30, 31]. The asymmetry originates from the circulation of the supercurrent around the vortex core and

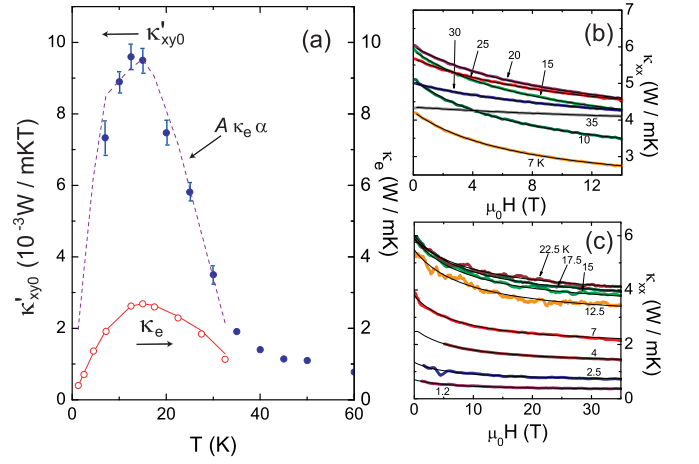


FIG. 2: (color online) (a)  $T$  dependence of the weak-field slope  $\kappa'_{xy0} \equiv \lim_{H \rightarrow 0} \kappa_{xy}/H$  (solid circles with error bars). As  $T$  falls below  $T_c$ ,  $\kappa'_{xy0}$  displays a steep increase to reach a peak at 18 K. For comparison, the quantity  $A\kappa_e\alpha$  (with  $A = 0.033$ , see below) is plotted as the dashed curve, and the electronic term  $\kappa_e$ , inferred from Eq. 2, is displayed as open circles. Curves of  $\kappa_{xx}$  vs.  $H$  at fixed  $T$  measured with thermocouples to 14 T (b) and with RuO<sub>x</sub> sensors to 35 T (c). In both, fits to Eq. 2 are shown as thin curves.

the Volovik effect [32]. The qp Hall current initially scales linearly with the vortex line density  $n_V = |B|/\phi_0$ , where  $B$  is the flux density and  $\phi_0$  the superconducting flux quantum. At large  $B$ , however, vortex scattering also reduces the mean-free-path of the qps (see below), resulting in a negative curvature in  $\kappa_{xy}(H)$ . In Fig. 1(c), the steady increase in curvature is seen as  $T$  decreases from 20 to 7 K.

Focusing on the weak- $H$  regime, we see that the sharp change at  $T_c$  in the qp Hall conductivity  $\kappa_{xy}$  is apparent when we plot the weak-field slope  $\kappa'_{xy0} \equiv \lim_{H \rightarrow 0} \kappa_{xy}/H$  (solid circles in Fig. 2(a)). As  $T$  decreases from 200 K to  $T_c$ ,  $\kappa'_{xy}$  increases slowly by a factor of  $\sim 3$ . At  $T_c$ ,  $\kappa'_{xy0}$  exhibits a sharp break in slope followed by a steeper rise to a peak that is  $\sim 5$  times larger than its value at  $T_c$  (curves of  $A\kappa_e\alpha$  and  $\kappa_e$  are discussed below).

We next turn to the diagonal term  $\kappa_{xx}(T, H)$ , which provides quantitative estimates of the electronic term  $\kappa_e$  and  $\ell_0$  independent of  $\kappa_{xy}$  (Fig. 2(b) and 2(c)). In the normal state, over the interval 250 to 40 K, the field dependence of  $\kappa_{xx}$  is undetectable with our sensitivity. Just below  $T_c$ , a weak  $H$  dependence becomes apparent (curve at 35 K). As  $T$  decreases, this rapidly evolves to a singular  $|B|$  dependence that characterizes the scattering of qps from pinned vortices in type-II superconductors in the clean limit ( $\ell_0 \gg \xi$ , where  $\xi$  is the coherence length).

The data in Fig. 2(b) and 2(c) fit well to the vortex-scattering expression (shown as thin curves) [22, 30, 31]

$$\kappa_{xx}(T, B) = \frac{\kappa_e(T)}{1 + \alpha(T)|B|} + \kappa_{ph}(T), \quad (2)$$

where  $\alpha(T) = \ell_0 \sigma_{tr}/\phi_0$  with  $\sigma_{tr}$  the vortex cross-section

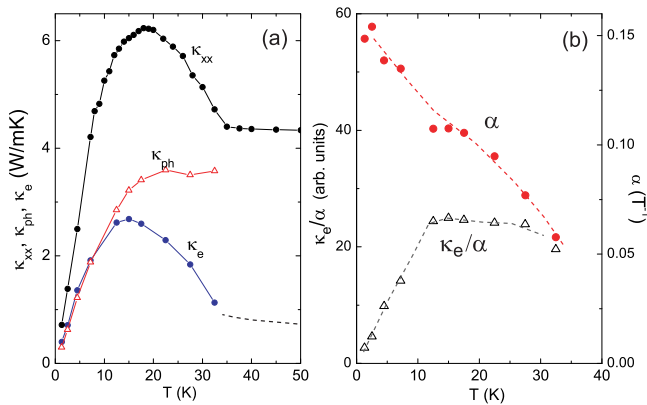


FIG. 3: (color online) (a) Comparison of  $\kappa_{xx}$  with  $\kappa_e$  and  $\kappa_{ph}$  inferred from fits of curves in Fig. 2(b) and 2(c) to Eq. 2. Above  $T_c$ ,  $\kappa_e$  is less than  $\frac{1}{5}\kappa_{xx}$ . Below  $T_c$ , however,  $\kappa_e$  increases rapidly to account for the entire anomaly in the observed  $\kappa_{xx}$ . Panel (b) displays  $\alpha = \ell_0\sigma_{tr}/\phi_0$  (solid circles) and  $\kappa_e/\alpha$  (open triangles) obtained from the fits. With  $\sigma_{tr} \sim 26 \text{ \AA}$ , we estimate that  $\ell_0 \simeq 1,200 \text{ \AA}$  at 2 K. The quantity  $\kappa_e/\alpha$  is a measure of the qp population below  $T_c$ .

presented to an incident qp. Equation 2 expresses the additivity of the zero- $H$  scattering rate ( $\sim \ell_0^{-1}$ ) and the scattering rate introduced by vortices  $\ell_v^{-1} = \sigma_{tr}nV$ . Because  $H_{c2} > 80 \text{ T}$ , the condensate amplitude is nearly unaffected by the applied  $H$ . Hence we can assume that  $\kappa_e(T)$  is nearly independent of  $H$ , and the dominant contribution to the observed  $H$  dependence arises from vortex scattering. We have assumed that the phonon term  $\kappa_{ph}$  has negligible  $H$  dependence, consistent with  $q\xi \ll 1$ , where  $q$  is the average phonon wave vector for  $T < T_c$ .

From the fits to the curves in Fig. 2, we have determined  $\kappa_e(T)$ ,  $\kappa_{ph}(T)$  and  $\alpha(T)$ . As shown in Fig. 3(a), the phonon term  $\kappa_{ph}$  (open triangles) decreases monotonically as  $T$  decreases below  $T_c$ . By contrast, the zero- $H$  electronic term  $\kappa_e$  rises to a broad maximum at 15 K and then falls. As evident, the monotonic profile of  $\kappa_{ph}$  implies that the peak in  $\kappa_{xx}$  (in zero  $H$ ) is entirely associated with  $\kappa_e$ . In turn, the large peak in  $\kappa_e$  demands a large qp population that survives to  $\sim \frac{1}{2}T_c$ .

The fits also yield estimates of  $\alpha = \ell_0\sigma_{tr}/\phi_0$  which we display in Fig. 3(b). As  $T$  decreases from 35 to 1.2 K,  $\alpha$  rises to  $3\times$  the value at  $T_c$ . This reflects primarily the increase in  $\ell_0$ . According to Cleary [31], the cross-section  $\sigma_{tr} \simeq \xi$ . With the estimate  $\xi \simeq 20 \text{ \AA}$  (from  $H_{c2} \sim 85 \text{ T}$ ), we find that  $\alpha$  at 1.2 K corresponds to  $\ell_0 \simeq 1,200 \text{ \AA}$ . This supports our assumption that  $\text{Ba}_{1-x}\text{K}_x\text{Fe}_2\text{As}_2$  is in the clean limit  $\ell_0 \gg \xi$  as has been widely reported. Since  $\kappa_e$  is proportional to  $\ell_0$ , a nominal picture of the  $T$  dependence of the qp population may be obtained from the ratio  $\kappa_e/\ell_0$ . This quantity is plotted as open triangles in Fig. 3(b). Initially,  $\kappa_e/\ell_0$  is nominally  $T$ -independent, but decreases linearly with  $T$  below 13 K.

The fits of  $\kappa_{xx}$  vs.  $H$  to Eq. 2 has allowed us to determine  $\kappa_e$ ,  $\kappa_{ph}$ , and  $\alpha$  independent of  $\kappa_{xy}$ . To show that these estimates are consistent with the thermal Hall

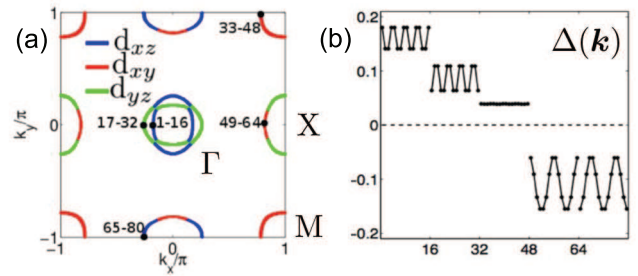


FIG. 4: (color online) Band structure (a) and SC gap function (b) for the 122 band structure around optimally hole-doped filling. The different dominant  $d$  orbital weights are plotted along the Fermi surface in (a) indicated by blue, green, and red. The pockets are divided into 80 momentum patches enumerated counterclockwise (a).

conductivity, we note that  $\kappa'_{xy0} \sim \ell_0^2$  should share the same  $T$  dependence as  $\alpha\kappa_e \sim \ell_0^2$ , in the semi-classical approximation. In Fig. 2(a), we have plotted  $A\kappa_e\alpha$  with the scale-factor  $A = 0.033$  (dashed curve) to compare it with the measured values of  $\kappa'_{xy0}$ . Within the uncertainty inherent in  $\kappa'_{xy0}$ , the  $T$  dependences may be seen to track each other quite well, especially between 12 and 35 K. Hence, both  $\kappa_{xx}$  and  $\kappa_{xy}$  indicate a large hole-like qp population that persists down to  $T \sim \frac{1}{2}T_c$ . Moreover, the values of  $\alpha \sim \ell_0$  inferred from  $\kappa_{xx}$  give a consistent description of the  $T$  dependences of both  $\kappa_e$  and  $\kappa'_{xy0}$ .

The experimental evidence of large low-lying hole-like qp weight we obtain from our thermal Hall measurement can be reconciled with a theoretical perspective on the problem. Starting from a simplified band structure fit for  $\text{Ba}_{1-x}\text{K}_x\text{Fe}_2\text{As}_2$  [33], the Fermi surface topology is schematically depicted in Fig. 4(a) in the unfolded Brillouin zone with 1 Fe atom per unit cell. As seen there, the  $d_{xz}$  and  $d_{yz}$  Fe orbitals dominate the hole pockets at  $\Gamma$ , while the third hole pocket at M is composed of  $d_{xy}$ . (The third hole pocket at M which also maps onto the  $\Gamma$  point in the folded Brillouin zone has been detected in ARPES being of nearly identical size and shape as one of the other hole pockets [21, 34].) The electron pockets at  $X = (\pi, 0)/(0, \pi)$  involve weights of all these three  $d$  orbitals. Assuming that the inter-pocket scattering is dominated by intra-orbital interactions, various theoretical approaches predict a significant gap anisotropy on the electron pockets as a consequence of frustrated electron-electron and electron-hole scattering [35, 36], while the hole pocket gaps are assumed rather homogeneous. In a 4 pocket scenario where the hole pocket at M is absent, it would hence be a natural guess that the weakest gap can be found on the electron pockets [35], and as a consequence that the thermal Hall signal in the SC phase should be electron-like. In contrast, the hole pocket at M significantly changes the situation: Fig. 4(b) shows the gap function  $\Delta(\mathbf{k})$  which we have computed by multi-orbital functional renormalization group [35, 37–39], with interaction parameters as chosen in [40]. To begin with,

we find the sign change from hole to electron pockets, as being characteristic for an  $s_{\pm}$  order parameter. The largest gap anisotropy is found on the electron pockets. However, we find the smallest amplitude to be located on the hole pocket at M. This is because most of the scattering of this pocket is governed by the subdominant inter-orbital repulsion scale, as only a small part of the electron pockets share the  $d_{xy}$  orbital content. In addition, the available phase space for qps is quite large on the pocket (or at least comparable to the other pockets), which is consistent with the dominant hole-like qp profile of the thermal Hall conductivity measurements.

We propose extending thermal Hall measurements beyond optimally doped  $\text{Ba}_{1-x}\text{K}_x\text{Fe}_2\text{As}_2$  will provide an incisive test to gain experimental insight into the nature of multi-band superconducting pairing mechanisms in general. For example, for further K doping we expect the hole-like profile to persist and become even more pronounced, as  $d$ -wave order can form and even give rise to nodes on the hole pockets [35]. Moving to the electron-doped side through Co doping should eventually remove the broad hole band giving rise to the hole pocket at M from the Fermi surface, by which the small gap regimes on the electron pockets should become the dominant contribution to low-energy charge carriers. We hence predict a sign change of the thermal Hall signal

as a function of doping. Similar trends may be triggered by stronger nodal propensity due to isovalent doping of the As-based compound by P, potentially giving rise to accidental nodes on the electron pockets [35, 41]. It may likewise be interesting to investigate the recently discovered iron chalcogenides such as  $\text{K}_x\text{Fe}_2\text{Se}_2$  [42, 43], where the potential role of hole-like carriers may be intimately linked to the competition between a possible  $s_{\pm}$  and gapped  $d$  wave order parameter [44–46]. As a result, it is likely that the properties of the quasiparticles extracted from heat transport will be valuable for understanding the pairing mechanism of multi-band superconductors.

We thank P. A. Lee, D.-H. Lee, S. Graser, D. Scalapino, B. A. Bernevig, and M. Z. Hasan for helpful discussions. The research at Princeton is supported by U.S. National Science Foundation (NSF) under Grant DMR-0819860. Research at IOP is supported by NSFC, 973 project of MOST and CAS of China. High-field experiments were performed at the National High Magnetic Field Laboratory, Tallahassee, a national facility supported by NSF, the Dept. of Energy and the State of Florida. RT is supported by an SITP fellowship by Stanford University.

<sup>†</sup>*Present address of JGC:* Advanced Science Institute, RIKEN, Saitama, Japan. <sup>‡</sup>*Present address of LL:* Dept. of Physics, University of Michigan, Ann Arbor, MI, USA.

- 
- [1] Y. Kamihara, T. Watanabe, M. Hirano, and H. Hosono, *J. Am. Chem. Soc.* **130**, 3296 (2008).  
 [2] Z. Ren *et al.*, *Chin. Phys. Lett.* **25**, 2215 (2008).  
 [3] G. F. Chen *et al.*, *Phys. Rev. Lett.* **100**, 247002 (2008).  
 [4] X. H. Chen, T. Wu, G. Wu, R. H. Liu, H. Chen, and D. F. Fang, *Nature* **453**, 761 (2008).  
 [5] C. de la Cruz *et al.*, *Nature* **453**, 899 (2008).  
 [6] D. N. Basov and A. V. Chubukov, *Nature Physics* **7**, 272 (2011).  
 [7] I. I. Mazin, D. J. Singh, M. D. Johannes, and M. H. Du, *Phys. Rev. Lett.* **101**, 057003 (2008).  
 [8] K. Kuroki *et al.*, *Phys. Rev. Lett.* **101**, 087004 (2008).  
 [9] V. Stanev, J. Kang, and Z. Tesanovic, *Phys. Rev. B* **78**, 184509 (2008).  
 [10] A. V. Chubukov, D. V. Efremov, and I. Eremin, *Phys. Rev. B* **78**, 134512 (2008).  
 [11] S. Graser, T. A. Maier, P. J. Hirschfeld, and D. J. Scalapino, *New Journal of Physics* **11**, 025016 (2009).  
 [12] P. J. Hirschfeld, M. M. Korshunov, and I. I. Mazin, *Rep. Prog. Phys.* **74**, 124508 (2011).  
 [13] Y. Nakai, K. Ishida, Y. Kamihara, M. Hirano, and H. Hosono, *J. Phys. Soc. Japan* **77**, 073701 (2008).  
 [14] K. Matano *et al.*, *Eur. Phys. Lett.* **87**, 27012 (2009).  
 [15] H. Fukazawa *et al.*, *J. Phys. Soc. Japan* **78**, 033704 (2009).  
 [16] M. Yashima *et al.*, *J. Phys. Soc. Japan* **78**, 103702 (2009).  
 [17] K. Hashimoto *et al.*, *Phys. Rev. Lett.* **102**, 207001 (2009).  
 [18] X. G. Luo *et al.*, *Phys. Rev. B* **80**, 140503 (2009).  
 [19] H. Ding *et al.*, *Eur. Phys. Lett.* **83**, 47001 (2008).  
 [20] L. Wray *et al.*, *Phys. Rev. B* **78**, 184508 (2008).  
 [21] H. Ding *et al.*, *J. Phys.: Condens. Matter* **23**, 135701 (2011).  
 [22] K. Krishana, J. M. Harris, and N. P. Ong, *Phys. Rev. Lett.* **75**, 3529 (1995).  
 [23] B. Zeini *et al.*, *Phys. Rev. Lett.* **82**, 2175 (1999).  
 [24] Y. Zhang, N. P. Ong, P. W. Anderson, D. A. Bonn, R. Liang, and W. N. Hardy, *Phys. Rev. Lett.* **86**, 890 (2001).  
 [25] K. Izawa, H. Yamaguchi, Y. Matsuda, H. Shishido, R. Settai, and Y. Onuki, *Phys. Rev. Lett.* **87**, 057002 (2001).  
 [26] Y. Onose, N. P. Ong, and C. Petrovic, *Europhys. Lett.* **80**, 37005 (2007).  
 [27] Y. J. Yan *et al.*, *Phys. Rev. B* **81**, 235107 (2010).  
 [28] J. Bardeen, G. Rickayzen, and L. Tewordt, *Phys. Rev.* **113**, 982 (1959).  
 [29] L. Tewordt, *Phys. Rev.* **129**, 657 (1963).  
 [30] A. C. Durst, A. Vishwanath, and P. A. Lee, *Phys. Rev. Lett.* **90**, 187002 (2003).  
 [31] R. M. Cleary, *Phys. Rev.* **175**, 587 (1968).  
 [32] G. Volovik, *JETP Lett.* **58**, 469 (1993).  
 [33] S. Graser, A. F. Kemper, T. A. Maier, H.-P. Cheng, P. J. Hirschfeld, and D. J. Scalapino, *Phys. Rev. B* **81**, 214503 (2010).  
 [34] L. Wray, R. Thomale, *et al.*, in preparation.  
 [35] R. Thomale, C. Platt, W. Hanke, and B. A. Bernevig, *Phys. Rev. Lett.* **106**, 187003 (2011).  
 [36] W. Hanke, C. Platt, and R. Thomale, *Ann. Phys. (Berlin)* **523**, 638 (2011).  
 [37] F. Wang, H. Zhai, Y. Ran, A. Vishwanath, and D.-H. Lee, *Phys. Rev. Lett.* **102**, 1047005 (2009).  
 [38] R. Thomale, C. Platt, J. Hu, C. Honerkamp, and B. A.

- Bernevig, Phys. Rev. B **80**, 180505 (2009).
- [39] C. Platt, C. Honerkamp, and W. Hanke, New J. Phys. **11**, 055058 (2009).
- [40] R. Thomale, C. Platt, W. Hanke, J. Hu, and B. A. Bernevig, Phys. Rev. Lett. **107**, 117001 (2011).
- [41] K. Kuroki, H. Usui, S. Onari, R. Arita, and H. Aoki, Phys. Rev. B **79**, 224511 (2009).
- [42] J. Guo *et. al.*, Phys. Rev. B **82**, 180520 (2010).
- [43] M. H. Fang *et. al.*, Eur. Phys. Lett. **94**, 27009 (2011).
- [44] F. Wang, F. Yang, M. Gao, Z.-Y. Lu, T. Xiang, and D. H. Lee, Eur. Phys. Lett. **93**, 57003 (2011).
- [45] T. A. Maier, S. Graser, P. J. Hirschfeld, and D. J. Scalapino, Phys. Rev. B **83**, 100515 (2011).
- [46] C. Fang, Y.-L. Wu, R. Thomale, B. A. Bernevig, and J. Hu, Phys. Rev. X **1**, 011009 (2011).